Comparative Evaluation of Modulation Methods for a Three-Phase/Switch Buck Power Factor Corrector Concerning the Input Capacitor Voltage Ripple

Martina Baumann
Vienna University of Technology
Dept. of Electrical Drives and Machines
Gusshausstrasse 27/E372
A–1040 Vienna/Austria
Phone: +43-1-58801-37225
Fax: +43-1-58801-37298
martina.baumann@tuwien.ac.at

Johann W. Kolar
Swiss Federal Institute of Technology (ETH) Zurich
Power Electronics and Electrometrology Laboratory
ETH-Zentrum/LEM/ETL H22
CH–8092 Zurich/Switzerland
Phone: +41-1-6322834
Fax: +41-1-6321212
kolar@lem.ee.ethz.ch

Abstract **– For a three-phase three-switch buck-type PWM rectifier with unity power factor the rms value of the input filter capacitor voltage ripple is calculated for different modulation methods. A modulation method being optimal concerning the occurring switching losses and the rms value of the capacitor voltage ripple is identified and guidelines for the dimensioning of the input filter are derived.**

I Introduction

For the realization of three-phase PWM rectifier systems with sinusoidal input current usually boost-type converter topologies with impressed output voltage lying above the peak value of the line-to-line mains voltage were investigated in the literature [1], [2]. However, in connection with applications requiring a controllability of the output voltage, e.g., battery charging [1], the supply of six-step-inverters with variable DC-link voltage [3], process power supplies, etc., buck-type converter structures which allow a variation of the output voltage in a wide range and an output current limitation in the case of a short circuit of the load gain more and more importance.

Buck-type PWM rectifier systems show a discontinuous behavior of the input current. Therefore, a LC low-pass input filter has to be provided for suppressing the switching frequency components in the mains current. However, this does result in additional capacitive reactive power drawn from the mains and/or does impair the power factor of the recifier at low output power. The aim of the input filter dimensioning is therefore the limitation of the capacitance of the filter to a value as low as possible and/or the selection of a maximum pulse frequency.

For the buck-type PWM rectifier system depicted in **Fig. 1** [4] the switching power loss is influenced by the switching state sequence within one pulse period and/or by the line-to-line mains voltage being switched at the transition to a subsequent switching state [5]. Three classes of switching state sequences can be identified showing a ratio of the average values of switching power losses of $1 : \sqrt{3} : 2$. Therefore, for equal switching losses pulse frequencies showing a ratio $1 : 1/\sqrt{3} : 1/2$ have to be selected [7], [8]. However, the switching state sequence takes influence not only on the switching losses but also on the time behavior of the input filter capacitor voltage ripple. Therefore, the ratio of the pulse frequencies does not provide the full scope concerning the resulting capacitor voltage ripple.

In this paper the rms values of the input capacitor voltage ripple resulting for the different classes of switching state sequences at equal switching losses are calculated and comparatively evaluated. This gives a basis for the dimensioning of the input filter capacitors. In **section II** the basic principle of operation of the unidirectional three-phase/switch buck-type PWM rectifier system and the calculation of the switching losses are described briefly. Based on this, the time behavior of the input capacitor voltage ripple is analyzed in **section III**. There, the local ripple peak values of the phases, and the local rms value of the ripple are calculated analytically [6]. Integrating the local rms value over a mains period leads to a simple analytical expression for the global rms value of the voltage ripple, which can be used to evaluate the modulation methods in connection with the envelope of the capacitor voltage ripple which does define the local peak values of a capacitor phase voltage. Finally, the ripple characteristics are comparatively evaluated in **section IV** for the different modulation methods, and it is shown that the modulation method having minimum switching losses also leads to a minimum rms value of the input capacitor voltage ripple.

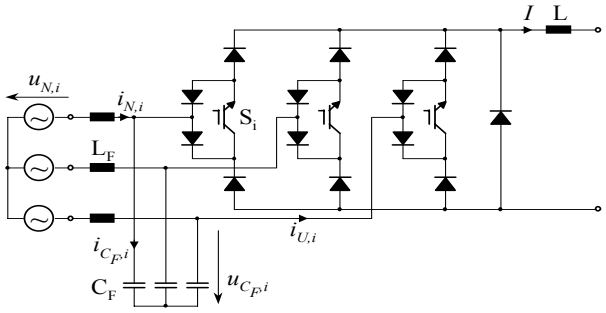

Fig. 1: Structure of the power circuit of the three-phase/switch buck power factor corrector.

II Basic Principle of Operation

In the following, the basic principle of operation of the system depicted in Fig.1 is briefly explained. Based on the investigation of the conducting states the related current space vectors are calculated, and several possibilities for arranging the switching states within one pulse period are analyzed.

A Assumptions and Definitions

For the sake of simplicity we assume for the further considerations:

- a purely sinusoidal shape of the filter capacitor voltage and/or $u_{C_F,i} \approx u_{N,i}$ where the mains voltage $u_{N,i}$ is defined as

$$\begin{aligned} u_{N,R} &= \hat{U}_N \cos(\omega_N t), \\ u_{N,S} &= \hat{U}_N \cos(\omega_N t - 2\pi/3), \\ u_{N,T} &= \hat{U}_N \cos(\omega_N t + 2\pi/3), \end{aligned} \tag{1}$$

and/or in space vector notation as

$$\underline{u}_N = \hat{U}_N \exp(\jmath\,\varphi_N), \tag{2}$$

($\varphi_N = \omega_N t$, ω_N denotes the mains angular frequency), and

- the inductor current I to be constant and impressed.

According to $u_{C_F,i} \approx u_{N,i}$ we will neglect

- the fundamental voltage drop $\jmath\,\omega_N L_F\,\underline{i}_N$ across the input filter inductors L_F, and furthermore, we do neglect
- the mains current ripple, i.e., we will consider the mains current $i_{N,i}$ as being equal to the fundamental of the rectifier input current, $i_{U,(1),i} \approx i_{N,i}$.

Remark: The space vector related to a triple of phase quantities is calculated according to the defining equation (shown for the example of the buck PFC input current)

$$\underline{i}_U = \frac{2}{3}\left(i_{U,R} + \underline{a}\,i_{U,S} + \underline{a}^{\,2}\,i_{U,T}\right) \qquad \underline{a} = \exp\left[\jmath\,2\pi/3\right]. \tag{3}$$

In summary, for an ideally sinusoidal shape of the mains phase voltage we would like to form a fundamental of the rectifier input current lying in phase with the mains phase voltage ($\varphi_U \approx \varphi_N$)

$$\underline{i}^{\,*}_{U,(1)} = \hat{I}_{U,(1)} \exp\left[\jmath\varphi_U\right] \approx \underline{i}_N \tag{4}$$

where the index (1) does denote the fundamental component; the switching frequency components of rectifier input phase currents $i_{U,i}$ are largely suppressed by the input filter (L_F, C_F in Fig. 1).

B Conduction States and Current Space Vectors

Due to the phase symmetry of the converter structure and due to the (assumed) symmetry of the mains voltage system, the investigation can be constrained to a $\frac{\pi}{3}$-wide interval of the mains period. At the case at hand we will consider the interval $\varphi_U \in (0; \frac{\pi}{3})$ being characterized by a relation of the mains phase voltages of $u_{N,R} > u_{N,S} > u_{N,T}$.

The characterization of the switching state of the buck rectifier is given by the combination $j = (s_R\,s_S\,s_T)$ of the phase switching functions. For the denomination of the switching states of the power transistors S_i, $i = R, S, T$, switching functions s_i are used in the following, where $s_i = 0$ denotes the off-state, and $s_i = 1$ denotes the on-state. The conduction states of the rectifier system are shown in **Fig. 2**, **Fig. 3** shows the related input current space vectors which are calculated based on (3).

E.g., for $s_R = 1$, $s_S = 1$ and $s_T = 0$ there results a positive current $+I$ in phase R and a negative current $-I$ in phase S due to $u_{N,R} > u_{N,S}$, and according to (3) an input current space vector $\underline{i}_{U,(110)} = \frac{2}{\sqrt{3}}\,I\,\exp\left[-\jmath\,\frac{\pi}{6}\right]$ is formed at the input. If all power transistors S_i, $i = R, S, T$, are in the on-state, $j = (111)$, the system corresponds to a three-phase diode bridge. Due to $u_{N,R} > u_{N,S} > u_{N,T}$ there follows $i_{U,R} = +I$ and $i_{U,T} = -I$. In this case, the generated input current space vector $\underline{i}_{U,(111)} = \frac{2}{\sqrt{3}}\,I\exp\left[\jmath\,\frac{\pi}{6}\right]$ is equal to the space vector $\underline{i}_{U,(101)}$. Since no difference in the input phase current behavior is given, the switching state $j = (101)$ or $j = (111)$ can be used for achieving $i_{U,R} = +I$, $i_{U,S} = 0$ and $i_{U,T} = -I$.

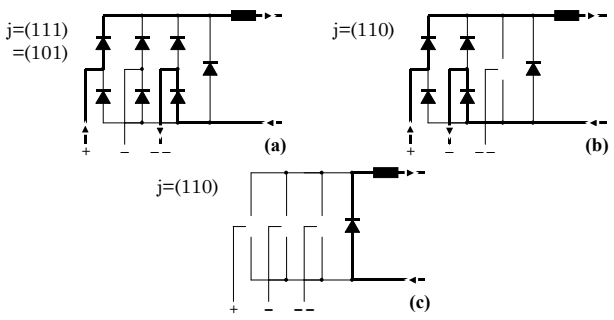

Fig. 2: Conduction states of the buck rectifier valid for $u_{N,R} > 0 > u_{N,S} > u_{N,T}$. The current flow is indicated by a bold line, the power transistors are not shown explicitly for the sake of clearness.

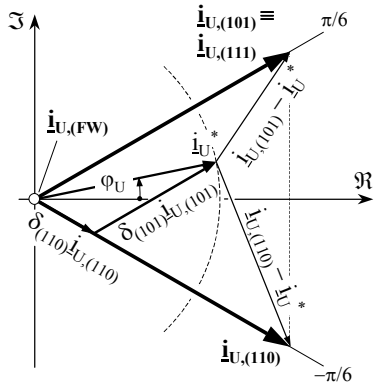

Fig. 3: Input current space vectors $\underline{i}_{U,j}$ according to Fig. 2 and to (3), valid for $u_{N,R} > 0 > u_{N,S} > u_{N,T}$ and/or $\varphi_U \in (0; \frac{\pi}{3})$, approximation of the reference vector $\underline{i}^{\,*}_U$ via neighboring current space vectors, and deviation between reference and actual space vectors.

C Switching State Sequences

For the formation of a given reference value $\underline{i}^{\,*}_U$ of the input current and/or of a related mains current $\underline{i}_N \approx \underline{i}^{\,*}_U$ only the space vectors lying in the immediate neighborhood of $\underline{i}^{\,*}_U$ are incorporated into the switching state sequence in order to achieve a deviation as small as possible between reference and actual space vectors. In general, the switching states valid within one pulse (half) period have to be arranged in such a manner that a minimum number of switching transitions of the power transistors and/or minimum switching losses do occur[1].

There are several possibilities for arranging the switching states within one pulse (half) period. The switching states can either be arranged symmetrically (cf. **Tab. 1**, sequences 1 and 2) or asymmetrically (cf. Tab. 1, sequence 3) to the middle of the pulse period. Besides that, the free-wheeling state can either be placed in the middle of a pulse half period (cf. sequence 2) or at the beginning and/or at the end of a pulse half period, respectively (cf. sequence 1). In Tab. 1 only switching state sequences employing a clamped power transistor within a $\frac{\pi}{3}$-wide interval are given, however, one also has the possibility to use the switching state $j = (000)$ as a free-wheeling state. The symmetric modulation methods presented here do not show a difference regarding to the number of switching transitions

[1] For $\varphi_U \in (0; \frac{\pi}{6})$ the space vectors $i_{U,(101)} \equiv i_{U,(111)}$, $i_{U,(110)}$ and $i_{U,(FW)}$ are employed. $j = (FW)$ does denote the free-wheeling state, $(FW) = (100)$, (010), (001), (000).

Seq.	j_1	j_2	j_3	j_4	j_5	j_6	$S_{cl.}$
1	(111)	(110)	(100)	(100)	(110)	(111)	S_R
2	(110)	(100)	(101)	(101)	(100)	(110)	S_R
3	(111)	(110)	(100)	(111)	(110)	(100)	S_R

Tab. 1: Switching state sequences available for two subsequent pulse half periods valid within $\varphi_U \in (0; \frac{\pi}{6})$, $S_{cl.}$ does denote the power transistor being clamped in the on-state.

(if those occurring at zero current are neglected), for switching state sequence 3 there are more switching actions necessary, i.e., phase T does show twice the switching frequency as for method 1 and 2, switching of phase S is not influenced (considering a mains phase voltage condition $u_{N,R} > 0 > u_{N,S} > u_{N,T}$). And, as shown in the following, all modulation methods result in different switching losses.

D Switching Losses

For the sake of simplicity we assume (i) the switching energy loss w to be proportional to the switched voltage $u(t)$ (the proportional relationship is represented by a constant of proportionality k), and (ii) a constant switched current I (as impressed by the inductor L).

The average value of the global switching energy loss (related to a mains period T_N) can then be calculated from the sum of the local switching energy losses $w(t)$ (related to a pulse period T_P) of all power transistors S_i incorporated into the switching actions via

$$W = \frac{1}{T_N} \int_0^{T_N} \sum_i w_{S_i}(t) \mathrm{d}t. \tag{5}$$

Investigating e.g. sequence 1 in Tab. 1 we have: At the transition from the switching state $j = (111)$ to $j = (110)$ the power transistor S_T has to be turned off at a voltage $u_{C_F,ST}$. At the following transition $j = (110) \rightarrow j = (100)$ the power transistor S_S has to be turned off at a voltage $u_{C_F,RS}$. In the subsequent pulse half period the power transistors S_S, S_T have to be switched on again at the same voltages, but in reverse order. The switching energy loss within a pulse period can then be calculated as

$$w(t) = k\,I\,(u_{C_F,ST}(t) + u_{C_F,RS}(t)) = k\,I\,u_{C_F,RT}(t) \tag{6}$$

with $k = k_{\mathrm{on}} + k_{\mathrm{off}}$. Due to the symmetry of the feeding AC mains and the rectifier topology the integration can be constrained to an interval $\varphi_U \in (0; \frac{\pi}{6})$. Based on (6) one receives for the average value of the global switching power loss within one mains period

$$P = W\,f_P = \tag{7}$$
$$= \frac{1}{\frac{\pi}{6}} \int_0^{\frac{\pi}{6}} k\,f_P\,I\,u_{C_F,RT}(\varphi_U)\,\mathrm{d}\varphi_U = \frac{3\sqrt{3}}{\pi} k\,f_P\,I\,\hat{U}_N.$$

The switching power losses for the switching sequences shown in Tab. 1 are given in **Tab. 2**. With respect to Tab. 2 one can see immediately that the modulation method with the free-wheeling state lying at the beginning and/or at the end of one pulse half period, respectively, are advantageous over other switching state sequences regarding the switching losses. Since the modulation method takes influence not only on the switching losses but also on the rms value of the input capacitor voltage ripple, the input filter rms value is calculated for the different modulation methods in the following section. This does provide the basis for the dimensioning of the input filter capacitor.

Seq.	$P/(f_P\,k\,I\,\hat{U}_N)$
1	$3\sqrt{3}/\pi$
2	$9/\pi$
3	$6\sqrt{3}/\pi$

Tab. 2: Average value of the switching power losses for the switching states sequences given in Tab. 1.

III Ripple of the Input Filter Capacitor Voltage

A Analytically Closed Calculation

As a quality functional the integral (related to a mains period) of the square of the deviation

$$\Delta\underline{u}_{C_F} = \underline{u}_{C_F} - \underline{u}^*_{C_F} \tag{8}$$

between the input capacitor voltage actual and reference value, or the rms value of the input filter capacitor voltage, respectively, is selected

$$Q = \Delta U^2_{C_F,RST,rms} = \frac{1}{T_N} \int_{T_N} \Delta u^2_{C_F,RST,rms}(\tau)\mathrm{d}\tau\ . \tag{9}$$

For the calculation of the quality functional Q one can choose a simple equivalent circuit of the system (cf. **Fig. 4**) according to

$$C_F \frac{\mathrm{d}\underline{u}_{C_F}}{\mathrm{d}t} = \underline{i}_N - \underline{i}_U. \tag{10}$$

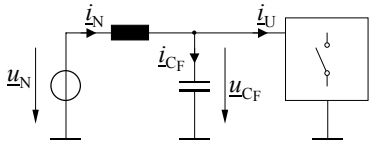

Fig. 4: Space vector equivalent circuit of the system AC side.

The space vector of the input filter capacitor voltage ripple $\Delta\underline{u}_{C_F}$ can be calculated via

$$\frac{\mathrm{d}\Delta\underline{u}_{C_F}}{\mathrm{d}t} = \frac{1}{C_F}(\underline{i}_U - \underline{i}^*_U) \tag{11}$$

with

$$C_F \frac{\mathrm{d}\underline{u}^*_{C_F}}{\mathrm{d}t} = (\underline{i}_N - \underline{i}^*_U) \tag{12}$$

and the approximation of the circular trajectory of the reference voltage space vector by the local tangent

$$\begin{aligned} \underline{i}^*_U(\tau) &= \underline{i}_N(\tau) - \jmath\omega C_F \underline{u}^*_N(\tau) \\ \underline{u}^*_N(\tau + t_\mu) &= \underline{u}^*_N(\tau) + \jmath\omega t_\mu \underline{u}^*_N(\tau), \end{aligned} \tag{13}$$

where t_μ denotes the local time being counted within one pulse half period. Incorporating the neighboring current space vectors with proper on-time δ_j in the formation of the input current reference value (cf. Fig. 3) one receives

$$\underline{i}^*_U = \underline{i}_{U,(110)}\,\delta_{(110)} + \underline{i}_{U,(101)}\,\delta_{(101)} \tag{14}$$

with

$$\begin{aligned}\delta_{(111)} &= M\,\sin(\pi/3+\varphi_U),\\ \delta_{(110)} &= M\,\sin(\pi/3-\varphi_U),\\ \delta_{(111)} &= 1-\delta_{(111)}-\delta_{(110)},\end{aligned} \tag{15}$$

where M denotes the modulation index of the buck rectifier,

$$M=\frac{\hat{I}_N}{I} \qquad M\in[0;1]\ . \tag{16}$$

With this, the local rms value (related to a pulse (half) period) of the input capacitor voltage ripple can be calculated via

$$\Delta u^2_{C_F,RST,rms}(\tau)=\frac{2}{T_P}\int_{t_\mu=0}^{t_\mu=\frac{1}{2}T_P}\frac{3}{2}|\Delta\underline{u}_{C_F}|^2\mathrm{d}t_\mu \tag{17}$$

according to

$$\Delta u^2_{C_F,R}(t_\mu)+\Delta u^2_{C_F,S}(t_\mu)+\Delta u^2_{C_F,T}(t_\mu)=\frac{3}{2}|\Delta\underline{u}_{C_F}|^2. \tag{18}$$

For the calculation of the global rms value (being set equal to the quality functional Q) related to a mains period we receive with sufficiently good approximation for high pulse frequency

$$\begin{aligned}Q &= \Delta U^2_{C_F,RST,rms}=\\ &= \frac{1}{T_N}\int_{T_N}\frac{2}{T_P}\int_{t_\mu=0}^{t_\mu=\frac{1}{2}T_P}\frac{3}{2}|\Delta\underline{u}_{C_F}|^2\,\mathrm{d}t_\mu\,\mathrm{d}\tau\\ &= \frac{1}{T_N}\int_{T_N}\Delta u^2_{C_F,RST,rms}(\tau)\,\mathrm{d}\tau,\end{aligned} \tag{19}$$

which allows a simple analytically closed calculation of the rms value of input capacitor voltage ripple.

B Trajectory of the Voltage Space Vector

In the following, for one characteristic input current space vector $\underline{i}^*_U$ the trajectories of the space vector of the input capacitor voltage ripple $\Delta\underline{u}_{C_F}(t_\mu)$ are given for the different switching state sequences according to Tab. 1.

(1) Symmetric Switching State Sequences
Considering the different switching state sequences given in Tab. 1 one can calculate the voltage space vectors $\Delta\underline{u}_{C_F,t_{\mu_i}}$ in dependency on the global time τ. E.g., for switching state sequence 1 one receives

$$\Delta\underline{u}_{C_F,t_{\mu_1}}(\tau)\ =\ \delta_{(111)}\left[\underline{i}_{U,(111)}-\underline{i}^*_U(\tau)\right]\frac{T_P}{2C_F}, \tag{20}$$

$$\Delta\underline{u}_{C_F,t_{\mu_2}}(\tau)\ =\ \delta_{(110)}\left[\underline{i}_{U,(110)}-\underline{i}^*_U(\tau)\right]\frac{T_P}{2C_F}+\Delta\underline{u}_{C_F,t_{\mu_1}}(\tau),$$

or

$$\begin{aligned}\frac{1}{u_n}\Delta\underline{u}_{C_F,t_{\mu_1}} &= \Delta u_{C_F,t_{\mu_1},\alpha}+\jmath\,\Delta u_{C_F,t_{\mu_1},\beta}=\\ &= \frac{1}{2}\,\delta_{(111)}\left[\sqrt{3}\,\delta_{(100)}+\jmath\,(1-\delta_{(111)}+\delta_{(110)})\right],\\ \frac{1}{u_n}\Delta\underline{u}_{C_F,t_{\mu_2}} &= \Delta u_{C_F,t_{\mu_2},\alpha}+\jmath\,\Delta u_{C_F,t_{\mu_2},\beta}=\\ &= \frac{1}{2}\,\delta_{(100)}\ \left[\sqrt{3}\,(\delta_{(110)}+\delta_{(111)})+\jmath\,(\delta_{(111)}-\delta_{(110)})\right],\end{aligned} \tag{21}$$

respectively, with (11), (14) and Fig. 3, and

$$u_n=\frac{\sqrt{3}\,T_P\,I}{4\,C_F}. \tag{22}$$

In **Fig. 5**(a) the trajectory of the space vector of the input capacitor voltage ripple $\Delta\underline{u}_{C_F}(t_\mu)$ is shown with reference to a current reference value i^*_U as given in Fig. 3 for modulation method 1. In Fig. 5(b) the trajectory is depicted for modulation method 2 showing the same shape but a different position as compared to the trajectory of modulation method 1, which results in different time behavior of the capacitor voltage ripple.

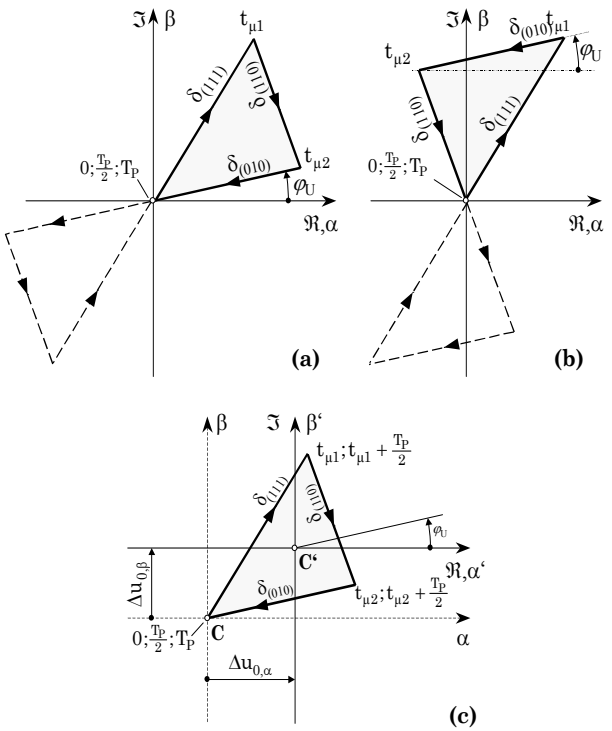

Fig. 5: Trajectory of the space vector $\Delta\underline{u}_{C_F}(t_\mu)$ within one pulse period, modulation methods 1: **(a)**, 2: **(b)**, and 3: **(c)**.

(2) Asymmetric Switching State Sequence
The trajectory of the space vector of the input capacitor voltage ripple for an asymmetric switching state sequence (cf. sequence 3 in Tab. 1) differs from trajectories of symmetric switching state sequences concerning its position relative to the origin (cf. **Fig. 5**(c)). For achieving the necessary condition of a local mean value of the capacitor voltage equal to zero (which does result automatically for a symmetric switching state sequence and/or symmetric ripple trajectory) one has to properly position the trajectory of the asymmetric switching state sequence (by proper system control) with reference to the origin. Accordingly, an offset ($\Delta u_{0,\alpha};\Delta u_{0,\beta}$ as shown in Fig. 5(c)) does occur in a way that

$$\frac{2}{T_P}\int_{t_\mu=0}^{t_\mu=\frac{1}{2}T_P}\left[\Delta u_{C_F,R}(t_\mu)+\Delta u_{C_F,S}(t_\mu)+\Delta u_{C_F,T}(t_\mu)\right]\mathrm{d}t_\mu=0$$

is fulfilled. Then, the center point C' is guided along a circle within a mains period and the trajectoy of the corner C does

differ from a circular shape. For the following calculation we, however, will assume a circular movement of C for the calculation of the rms value of the input filter capacitor voltage ripple in a first step in order to avoid involved analytical calculations. This does provide only a rough estimation of the actual performance of the modulation method, but is justified later on in Fig. 6 which does identify another modulation method as optimal for practical application. This picture would not be changed by a more accurate calculation.

C RMS Value of the Input Voltage Ripple

In the following, the rms value of the input voltage ripple for the different modulation schemes according to Tab. 1 is calculated via (19). For denoting the results the numbers of the switching states sequences are given as indices, e.g., index 1 for switching state sequence 1 in Tab. 1,

$$\Delta U^2_{C_F,RST,rms,1} = \tag{23}$$
$$= \frac{M^2}{128\pi}\left(-64M - 120\sqrt{3}M + 9\sqrt{3}M^2 + 48\pi + 36M^2\pi\right),$$

$$\Delta U^2_{C_F,RST,rms,2} = \tag{24}$$
$$= \frac{M^2}{128\pi}\left(-72\sqrt{3} - 160M - 27\sqrt{3}M^2 + 72\pi + 36M^2\pi\right),$$

$$\Delta U^2_{C_F,RST,rms,3} = \frac{M^2}{128\pi}\left(12\pi - 64M + 9M\pi\right). \tag{25}$$

In the sense of making a fair comparison of different modulation schemes, the pulse frequency f_P has to be modulated in such a manner that the average value of the switching power losses (cf. section D) related to a mains period is the same for all modulation methods. According to Tab. 2 one has to reduce the switching frequency for modulation method 2 by a factor of $\sqrt{3}$, and for modulation method 3 by a factor of 2, in order to achieve the same switching power loss as compared to modulation method 1. The corrected rms values of the input filter capacitor voltage in dependency on the modulation index M of the buck rectifier is given in **Fig. 6**. With this, the value of the input filter capacitor can be selected as being necessary for obtaining a given (maximum) rms value of the input voltage ripple.

D Time Behavior and Envelope of the Input Voltage Ripple

The knowledge about the time behavior and about the envelope of the input filter capacitor voltage ripple is useful in connection with the dimensioning of the input filter, because the rms value $\Delta U_{C_F,RST,rms}$ only provides an integral information about the ripple voltage time behavior. In the following, the time behavior of the input voltage ripple in phase R which is calculated based on the equations given in section A (cf. (20) for modulation method 1) is given for the following system operating parameters (which are typical, e.g, for a system application as front-end of a high-power telecommunications power supply module):

$$\begin{array}{llll} P_0 & = 5\,\mathrm{kW} & U_{N,ph} & = 210\,\mathrm{V} \\ U_0 & = 400\,\mathrm{V} & C_F & = 4\,\mu\mathrm{F} \\ I & = 12.5\,\mathrm{A} & f_P & = 20\,\mathrm{kHz} \end{array}$$

There, the modulation index follows as $M = 0.9$ according to (16). The fundamental component is assumed as $u_{N,R,(1)} = \hat{U}_N \cos(\varphi_U)$ (cf. (1)). The calculated time behavior is shown in **Figs. 7** (a)–(c), the voltage scale can be calculated based on (22), for modulation method 1 one receives for the reference value of the normalization

$$\Delta u_{n,1} = \frac{\sqrt{3}}{4}\,\frac{12.5\mathrm{A}}{4\mu\mathrm{F}\,10\mathrm{kHz}} = 67.7\,\mathrm{V}. \tag{26}$$

For modulation methods 2 the pulse frequency f_P has to be reduced according to section C, for the reference values there follows

$$\begin{array}{lcll} \Delta u_{n,2} & = & 117\,\mathrm{V} & \text{at } f_P = 11.5\,\mathrm{kHz} \\ \Delta u_{n,3} & = & 135\,\mathrm{V} & \text{at } f_P = 10\,\mathrm{kHz}. \end{array} \tag{27}$$

In **Fig. 8** the normalized envelopes of the input filter capacitor voltage ripple within an angle interval $\varphi_U \in (0;\pi/2)$ is given for the different modulation methods 1, 2, and 3, at modulation indices $M = 0.3/0.6/0.9$. The shape of the envelopes is approximately equal, but one has to point out the different scales of the normalized voltage, which already considers the different pulse frequencies for the different modulation methods according to Tab. 2 and section C.

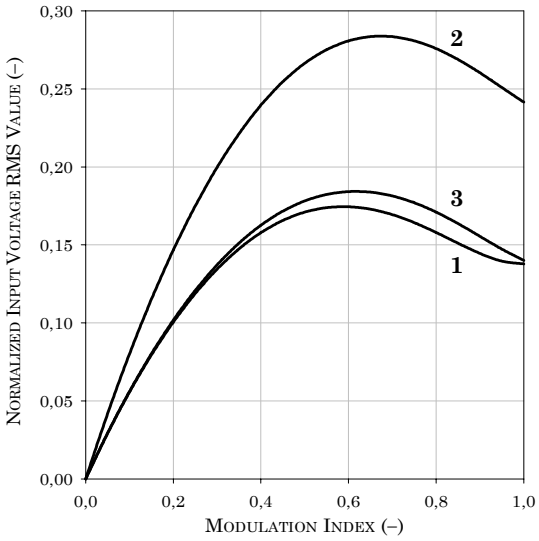

Fig. 6: Normalized rms value of the input capacitor voltage ripple in dependency on the modulation index M for modulation methods 1, 2, and 3.

IV Comparison of the Different Modulation Methods

With reference to Figs. 5 and (22) the results shown in Fig. 6 become immediately clear: For increasing pulse frequency there is a proportional decrease of the rms value of the input filter capacitor voltage ripple $\Delta U_{C_F,RST,rms}$, which shows a higher effect on the symmetric modulation method 2 than on the asymmetric modulation method 3 (cf. Fig. 5(b) and (c)). This is because of the size and the positioning of the corresponding ripple trajectories in the coordinate system which results in a lower instantaneous input capacitor voltage ripple rms value for the asymmetric modulation method 3. Even though modulation methods 1 and 3 show approximately equal rms values of the input capacitor voltage ripple, modulation method 1 is advantageous over modulation methods 3 due to the higher

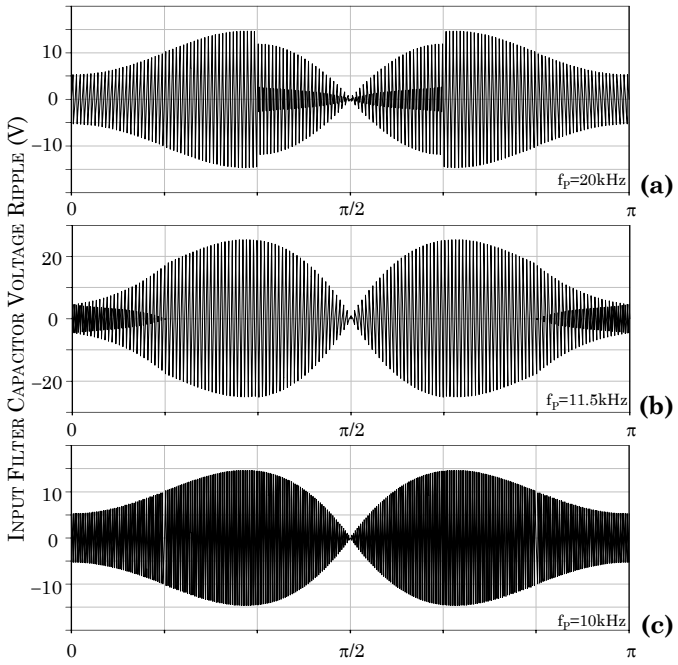

Fig. 7: Time behavior of the input capacitor voltage ripple $\Delta u_{C_F,R}$ in phase R for $M = 0.9$ for modulation methods 1, 2 and 3.

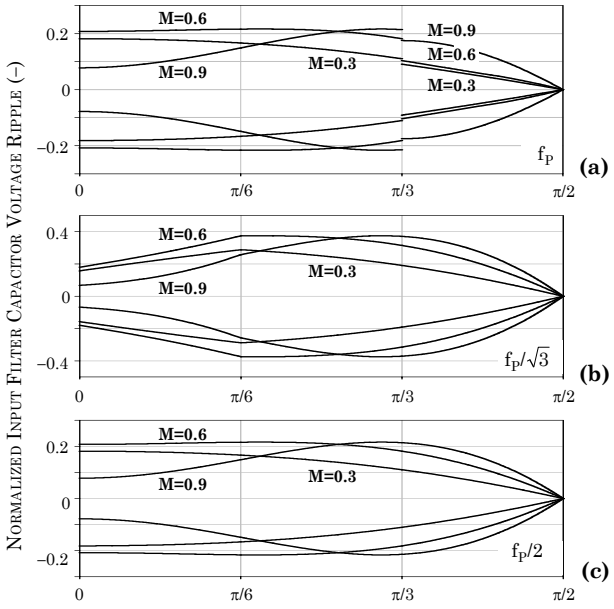

Fig. 8: Normalized input filter capacitor voltage ripple $\Delta u_{C_F,R}$ for different modulation indices M for modulation methods 1, 2 and 3.

switching frequency. For modulation method 1 a switching frequency being higher by a factor of 2 as compared to modulation method 3 can be selected for achieving equal global average switching losses, whereby the current harmonics occur at higher frequencies what results in a lower filtering effort.

V Conclusions

In this paper different modulation methods showing different average values of the switching losses (for equal switching frequency) were compared concerning the input capacitor voltage ripple. In order to obtain equal switching losses, the pulse frequencies have to be adjusted: the switching frequency has to be reduced for modulation method 2 (free-wheeling state in the middle of the pulse half period) by a factor of $\sqrt{3}$, and for modulation method 3 (asymmetric switching frequency) by a factor of 2 as compared to modulation method 1 (free-wheeling state at the beginning and/or at the end of a pulse half period).

The considerations show that switching state sequence 1 is advantageous over the other modulation methods concerning

- switching power loss,
- rms value of the input capacitor voltage ripple, and
- the pulse frequency.

Finally, we would like to point out that for the buck rectifier at hand the implementation of free-wheeling states with all power transistors in the off-state, $j = (000)$, is advantageous over modulation methods employing a switch clamped in the on-state for free-wheeling. Both modulation methods show equal switching losses, but implementing the free-wheeling by $j = (000)$ does avoid the occurrence of a sliding intersection of the input capacitor voltages which would result in a low-frequency mains current distortion, as will be decribed in detail in a future paper.

References

[1] **Mohan, N., Undeland, T.M., Robbins, W.P.:** *Power Electronics: Converters, Applications, and Design.* 2nd Edition. John Wiley & Sons, Inc. (1989).

[2] **Kolar, J.W., Zach, F.C.:** *A Novel Three-Phase Utility Interface Minimizing Line Current Harmonics of High-Power Telecommunications Rectifier Modules.* Proceedings of the 16th IEEE International Telecommunications Energy Conference, Vancouver, Canada, Oct. 30 - Nov. 3, pp. 367 - 374 (1994).

[3] **Baumann, M., Stögerer, F., Kolar, J. W., Lindemann, A.:** *Design of a Novel Multi-Chip Power Module for a Three-Phase Buck+Boost Unity Power Factor Line Interface Varying the DC Link Voltage of a Square-Wave VSI Drive.* 16th Applied Power Electronics Conference, March 4 - 8, Anaheim, U.S.A., Vol. 2, pp. 820 – 827 (2001).

[4] **Malesani, L., Tenti, P.:** *Three-Phase AC/DC PWM Converter with Sinusoidal AC Currents and Minimum Filter Requirements.* IEEE Transactions on Industry Applications, Vol. IA-23, No. 1 (1987).

[5] **Baumann, M., Drofenik, U., Kolar, J.W.:** *New Wide Input Voltage Range Three-Phase Unity Power Factor Rectifier Formed By Integration of a Three-Switch Buck-Derived Front-End and a DC/DC Boost Converter Output Stage.* 22nd IEEE International Telecommunications Energy Conference, Sept. 10 - 14, Phoenix, U.S.A., pp. 461 - 470 (2000).

[6] **Kolar, J.W., Ertl, H., Zach, F.C.:** *Analytically Closed Optimization of the Modulation Method of a PWM Rectifier System with High Pulse Rate.* Proceedings of the 17th International Conference on Intelligent Motion, Munich, Germany, June 25 - 29, pp. 370 - 381 (1990).

[7] **Halkosaari, T., Tuusa, H.:** *Optimal Vector Modulation of a PWM Current Source Converter According to Minimal Switching Losses.* Proceedings of the 31st IEEE Power Electronics Specialists Conference, June 18 - 23, Galway, Ireland, pp. 127 - 132 (2000).

[8] **Halkosaari, T., Tuusa, H.:** *Optimal Vector Modulation of a PWM Current Source Converter According to Minimum Distortion Constraint.* Proceedings of the International Power Electronics Conference, April 3 - 7, Tokyo, Japan, Vol. 2, pp. 958 - 963 (2000).